



HAL
open science

Modeling and Control of Pipeline Networks Supplied by Automated Irrigation Channels

Bojan Mavkov, Timm Strecker, Aaron Zecchin, Michael Cantoni

► **To cite this version:**

Bojan Mavkov, Timm Strecker, Aaron Zecchin, Michael Cantoni. Modeling and Control of Pipeline Networks Supplied by Automated Irrigation Channels. *Journal of Irrigation and Drainage Engineering*, 2022, 148 (6), 10.1061/(ASCE)IR.1943-4774.0001676 . hal-03695107

HAL Id: hal-03695107

<https://hal.science/hal-03695107>

Submitted on 13 Aug 2022

HAL is a multi-disciplinary open access archive for the deposit and dissemination of scientific research documents, whether they are published or not. The documents may come from teaching and research institutions in France or abroad, or from public or private research centers.

L'archive ouverte pluridisciplinaire **HAL**, est destinée au dépôt et à la diffusion de documents scientifiques de niveau recherche, publiés ou non, émanant des établissements d'enseignement et de recherche français ou étrangers, des laboratoires publics ou privés.

This material may be downloaded for personal use only. Any other use requires prior permission of the American Society of Civil Engineers. This material may be found at [https://doi.org/10.1061/\(ASCE\)IR.1943-4774.0001676](https://doi.org/10.1061/(ASCE)IR.1943-4774.0001676)

Modelling and control of pipeline networks supplied by automated irrigation channels

Bojan Mavkov¹, Timm Strecker², Aaron C. Zecchin³, and Michael Cantoni⁴

¹Lecturer-Researcher, Université Grenoble Alpes, CNRS, GIPSA-lab, F-38000, Grenoble, France, Email: bojan.mavkov@univ-grenoble-alpes.fr

²Research Fellow, Department of Electrical and Electronic Engineering, University of Melbourne, Parkville, VIC 3010, Australia, Email: timm.strecker@unimelb.edu.au

³Senior Lecturer, School of Civil, Environmental and Mining Engineering, University of Adelaide, SA 5005, Australia, Email: aaron.zecchin@adelaide.edu.au

⁴Professor, Department of Electrical and Electronic Engineering, University of Melbourne, Parkville, VIC 3010, Australia, Email: cantoni@unimelb.edu.au

ABSTRACT

A model-based approach to control system design is developed for regulating the discharge flows at the outlets of a pipeline network that is supplied by an irrigation channel. The open channel is also controlled automatically to regulate the supply-point water level. The hydraulic pressure at the source of the network is therefore dynamic when flow load varies. Regulation of the piped discharge flows is achieved by adjusting outlet control valves on the basis of the specified flow demand and sensor measurements. A blend of feedforward and feedback control is proposed. The steady-state behaviour of a non-linear distributed-parameter model of the network is used to determine the feedforward control action. The feedback control action is used to compensate for modelling error. The design of the feedback controller is based on a frequency-domain transfer function model of the system dynamics, and classical loop-shaping ideas. This model is obtained via the admittance matrix of linearized network equations. The synthesis of both centralized and decentralized feedback controller configurations is considered. Simulations that involve a non-linear distributed-parameter model of the network dynamics are used to illustrate controller performance.

INTRODUCTION

Consider a pipeline network, as illustrated in Figure 1. It is supplied at the downstream end of an irrigation channel without the aid of pumping. Suppose that the supply channel is automated in the sense that a feedback controller adjusts the channel

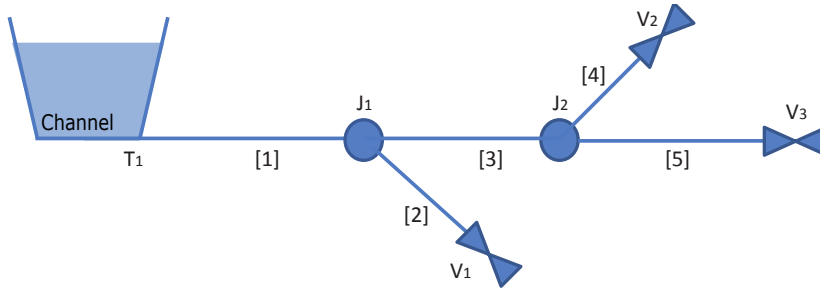


Fig. 1. Scheme of the water distribution network.

inflow to regulate the downstream water-level, as described in [Cantoni et al. \(2007\)](#) and references therein. The pressure head at the source of the pipeline network can therefore exhibit transient fluctuations according to the dynamic response of the automated channel to changes in the flow load. The valves are placed at the outlets of the outflow pipes and they are used to control the required flow by the fields that are irrigated. The proposed architecture is inspired by the low energy pipeline technology that is used to replace open earthen canals in the Murray Darling Basin, in order to improve irrigation water use efficiency by reducing losses due to seepage and evaporation [Koech and Langat \(2018\)](#).

The aim of the pipeline network control system is to regulate the discharge flows at end-user outlets, by the automatic adjustment of control valves, in response to changes of specified flow demand and sensor measurements. Feedback control action based on measured discharge flows can be used to compensate for transient variations in the pressure head at the interface with the automated channel dynamics, and for error in the static model used to set the valve openings that would yield the specified discharge flows in steady state.

An approach to the design of automatic pipeline network control systems is described in this paper. This includes the development of a modelling framework for the pipeline dynamics, given the automated irrigation channel dynamics at the source boundary. The design of both decentralized and centralized discharge valve controller configurations are considered. Understanding the interplay between the channel controller and the pipeline control system, and between the component valve controllers in the case of a decentralized configuration, is of interest in terms of the extent to which this may limit performance.

Several recent works are dedicated to modelling for the control of pipeline networks. Simplified lumped models of single pipeline systems can be found in [Matko et al. \(2000\)](#); [Bartecki \(2016\)](#); [Reddy et al. \(2010\)](#); [Razvarz et al. \(2019\)](#). Nonlinear models for the control of pipeline networks are presented in [Kaltenbacher et al. \(2017, 2018\)](#); [De Persis and Kallesoe \(2011\)](#). Control strategies for regulating hydraulic networks using pressure reducing valves are presented in [Prescott and Ulanicki \(2008\)](#); [Bermúdez et al. \(2021a\)](#); [Dai \(2021\)](#); [Galuppini et al. \(2020\)](#); [Bermúdez et al. \(2021b\)](#). Flow control of fluid in pipelines using torsional actuator placed on a motor pump is presented in [Razvarz et al. \(2020\)](#). These models are derived using simplified rigid wa-

ter column theory [Fox \(1977\)](#), which makes the system easy to analyze. However, this neglects the dynamic mechanisms that can lead to control system interactions of the kind mentioned above. Control strategies for hydraulic systems that consist of a single pipeline and one valve using predictive control based on infinite dimensional control theory that are using the water hammer equations are already presented in [Van Pham et al. \(2014\)](#); [Pham et al. \(2012\)](#).

In this paper, models are developed using the elastic water hammer theory. The corresponding non-linear distributed-parameter dynamics are described by coupled continuity and momentum equations [Chaudhry \(1979\)](#). The non-linear steady-state characteristics of this model are used to design the the feedforward control action for given steady flow demand. Linearization and finite-dimensional approximation based simplifications of the dynamics are used to design feedback controllers, which compensate for error in the result of the feedforward action. Importantly, the overall modelling framework enables analysis of interactions between the different components in the network.

A control-oriented model for the complete Multiple-Input and Multiple-Output (MIMO) pipeline network is developed. The approach is based on [Zecchin et al. \(2010, 2009\)](#); [Kim \(2008\)](#), where the transient model of an arbitrary pipeline network is obtained via the so-called Laplace-domain admittance matrix for a linearization of the continuity and momentum equations. Here these results are extended and adapted for control-oriented modelling. The fundamental equations are presented in the form of matrices with irrational transfer function entries. These transfer function matrices relate the controlled inputs and outputs of the network. This model captures the complete linearized dynamics of all small signal interaction between all the discharge points of the system and the channel.

To facilitate optimization based synthesis of feedback controllers, a method is developed for approximating the irrational transfer function MIMO model with a real rational transfer matrix, via a frequency-domain system identification technique [Ljung and Glad \(1994\)](#). The result is a model that is appropriate for \mathcal{H}_∞ loop-shaping [McFarlane and Glover \(1992\)](#) based synthesis of a centralized controller, taking into direct account the network coupling between the discharge valves. The outcome is compared with a decentralized controller configuration comprising just the proportional plus integral (PI) compensators used as design weights in the synthesis of the centralized controller.

Implementation of the decentralized controller is much simpler, in that the discharge flow measurements involved can be processed locally at each outlet, substantially reducing the need to communicate with a central host for controller implementation. In the decentralized case, only changes in the specified discharge demand and channel water-level set points need to be communicated globally. By contrast, the centralized approach requires discharge flow measurements to be gathered by a central host to determine the feedback control actions, for communication back to each outlet at a sufficient rate for the duration of transients induced by set point changes. It is shown that decentralized feedback control yields similar performance to a comparable centralized controller when action is limited to sufficiently low frequencies, as

elaborated subsequently.

The paper is organized as follows. In the next section, a physics based system model is developed. Next, the control methodology is first introduced to motivate the development of simplified models for controller synthesis. The synthesis of centralized and decentralized feedback controllers is then described. Finally, a case study of a pipeline network is presented and this model is used to validate the proposed methodology in simulations. Conclusions are given in the final section.

PHYSICAL SYSTEM MODELLING

The system of interest consists of a pipeline network, operating in the pressurized state (i.e., full). The network is supplied by an upstream automated irrigation channel. It is used to deliver requested flow to a set of end-users via downstream discharge control valves. The fundamental equations for the system are outlined below. The resulting non-linear distributed-parameter physical system model is used in the simulation studies presented in the paper.

Continuity and momentum equations

A model is developed here for the dynamics of a tree network of fluid lines (i.e., pipes) $\Lambda = \{1, 2, \dots, n_\Lambda\}$ and nodes $\mathcal{N} = \mathcal{N}_T \cup \mathcal{N}_J \cup \mathcal{N}_V = \{1, 2, \dots, n_\mathcal{N}\}$. Here \mathcal{N}_J denotes the set of junction nodes where fluid lines are connected, $\mathcal{N}_T = \{1\}$ is the ‘top’ (or ‘source’) node where the pipeline network is connected to the automated channel, and \mathcal{N}_V is the set of nodes associated with the discharge valves.

The dynamics of the fluid in the i -th pipeline is given combining the simplified continuity and momentum equations, under assumptions of negligible convective changes in velocity and constant liquid density [Chaudhry \(1979\)](#):

$$\begin{aligned} \frac{\partial h_i}{\partial t} + \frac{c^2}{gA_i} \frac{\partial q_i}{\partial x} &= 0, \quad x \in [0, L_i], \\ \frac{1}{A_i} \frac{\partial q_i}{\partial t} + g \frac{\partial h_i}{\partial x} + \frac{f q_i |q_i|}{2D_i A_i^2} &= 0, \quad x \in [0, L_i], \end{aligned} \quad (1)$$

for $i \in \Lambda$, where L_i (m) is the length of the pipe, $h_i(x, t)$ (m) is the pressure head and $q_i(x, t)$ (m^3/s) is flow in the pipeline at time t (s) and position x (m) along the pipe, c (m/s) is wave speed in the fluid, g (m/s^2) is the constant of gravitational acceleration, A_i (m^2) is cross-sectional area of the pipe, D_i (m) is the diameter of the pipe, and f is the friction coefficient.

Valve and irrigation channel models at the network boundaries

The homogeneous form for the valve flow equation is derived in [White \(2011\)](#). In the case when the valve discharges into air, the valve flow relation may be written as in [Chaudhry \(1979\)](#):

$$q = \gamma u_v \sqrt{2gh}, \quad (2)$$

where u_v (m^2) is the opening of the valve, which is the controlled input for the network, and γ is the coefficient of discharge of the valve. The opening of the valves is limited in the range of

$$0 \leq u_v \leq u_v^{\max}. \quad (3)$$

The uncontrolled dynamics of the upstream open channel that supplies the pipeline network can be modelled by the Saint-Venant equation (also known as the shallow water equations.) This set of equations stems from a law of mass conservation and a law of momentum conservation, and it is given by [Chaudhry \(2007\)](#):

$$\begin{aligned} \frac{\partial A_c}{\partial t} + \frac{\partial q_c}{\partial x} &= 0, \quad x \in [0, L_c], \\ \frac{\partial q_c}{\partial t} + \left(\frac{gA_c}{B} - \frac{q_c^2}{A_c^2} \right) \frac{\partial A_c}{\partial x} + \frac{2q_c}{A_c} \frac{\partial q_c}{\partial x} + gA_c(S_f - \bar{S}) &= 0, \quad x \in [0, L_c], \end{aligned} \quad (4)$$

where $q_c(x, t)$ (m^3/s) is flow in the channel and $A_c(x, t)$ (m^2) is the wetted cross-sectional area at time t (s) and position x (m) along the channel, B (m) is the top width, S_f is the friction slope and \bar{S} is the mean bed slope.

The channel model above represents its open-loop behavior. Under the operation of a feedback controller, that automatically adjusts the upstream inflow to regulate the downstream water level on the basis of online measurements, it is possible to represent the channel by a much simpler model. Specifically, when feedback control action is limited to sufficiently low frequencies (i.e., control loop bandwidth limited to one-tenth of the dominant channel wave frequency), as also required to ensure critical closed-loop stability properties [Cantoni et al. \(2007\)](#), the behavior of the downstream water level h_T is approximated well by the following integrator-delay model [Cantoni et al. \(2007\)](#); [Weyer \(2001\)](#) :

$$\frac{dh_T}{dt}(t) = c_{in} q_{in}(t - \tau) - c_{out} (q_{out}(t) + d_{out}(t)). \quad (5)$$

In this model, the inflow q_{in} is determined by the feedback controller, q_{out} is the downstream channel flow load and d_{out} is the flow load associated with the pipe network. The constants τ , c_{in} and c_{out} are model parameters that can be determined from system identification experiments [Weyer \(2001\)](#). While model (5) described the open loop (uncontrolled) behaviour of the channel, the closed-loop response of h_T can be derived by taking into account the dynamics controller that determines q_{in} depending on h_T . This work involves a proportional plus integral (PI) controller of the kind used in practice [Cantoni et al. \(2007\)](#). When combined with (5), a model of the dynamic relationship between d_{out} and h_T is obtained. For the design of pipeline valve feedback controller and for the simulation, this simplified model is used for the boundary condition at the source of the network, as discussed further in subsequent sections.

Pipeline and network boundary conditions

Neglecting the losses, using the equation of mass conservation for the flows, and the energy equation for pressures in pipe ends connected to the same junction, the following equations hold at each junction node $j \in \mathcal{N}_J$ [Chaudhry \(2007\)](#):

$$q_{l(j)}(L_{l(j)}, t) - \sum_{i \in \Lambda(j)} q_i(0, t) = 0, \quad (6a)$$

$$h_{l(j)}(L_{l(j)}, t) = h_i(0, t), \quad i \in \Lambda(j). \quad (6b)$$

where $l(j) \in \Lambda$ denotes the index of the upstream fluid line connected to node j (of which there is only one as the network is tree), and $\Lambda(j) \subset \Lambda$ is the subset of downstream fluid lines connected to node j .

At each discharge valve node $j \in \mathcal{N}_V$, the following relationship holds, where as above $l(j) \in \Lambda$ denotes the index of the upstream fluid line that supplies the corresponding valve:

$$q_{l(j)}(L_{l(j)}, t) = \gamma_j u_{v,j}(t) \sqrt{2gh_{l(j)}(L_{l(j)}, t)}. \quad (7)$$

Finally, at the node $\mathcal{N}_T = \{1\}$, at which the network connects to the automated channel, the following holds where, as above, $\Lambda(1) \subset \Lambda$ denotes the subset of downstream fluid lines connected to the channel supply point:

$$q_i(0, t) = d_{\text{out}}(t) \quad \text{and} \quad h_i(0, t) = h_T(t), \quad i \in \Lambda(1). \quad (8)$$

As already mentioned, it is important to recall that there is an additional relationship between d_{out} and h_T corresponding to the dynamics of the automated channel, as discussed further in the next section.

CONTROL-ORIENTED MODELLING

As briefly discussed in the introduction, the control problem at hand is to regulate the network discharge flows to specified values, as required to meet end-user demand. There are two aspects to the control approach considered. The first corresponds to a feedforward (open-loop) control action. Specifically, the full non-linear distributed parameter model is used to determine the discharge control valve openings required in steady-state. To compensate for modelling error, and the disturbance associated with changes of the outflow from the automated supply channel, which leads to fluctuations in the pressure head at the source of the pipeline network, the second part is a feedback control action. This feedback control is based on flow sensor measurements at the outlets. The proposed approach to design the feedback controller is to use linearization of the full model. This results in a model that is more amenable to classical methods for feedback control system design. The corresponding steps are detailed in the rest of this section, as follows: (1) derivation of the equilibrium equations for determining the feedforward component of the control action; (2) linearization of the dynamics; (3) derivation of the MIMO transfer function for feedback controller design via the Laplace-domain admittance matrix of the linearized network model; and (4) rational approximation via a frequency-domain system identification method. Feedback controller synthesis on the basis of the resulting model is the topic of this work, where both centralized and decentralized feedback control configurations are considered.

Steady-state equations for feedforward control

Equations characterizing the steady-state are provided here for given constant values for the pipeline discharge flows $\bar{q}_{V,j}$, $j \in \mathcal{N}_V$, and the reference \bar{h}_T of the irrigation channel controller, which is the steady-state level because of the assumed integral action [Åström and Murray \(2010\)](#); [Cantoni et al. \(2007\)](#). Using (1), and the above boundary conditions, the following nonlinear system of steady-state pipeline network

equations hold at equilibrium, where the notation $l(j) \in \Lambda$ and $\Lambda(j) \subset \Lambda$ is as defined in the previous section, for $j \in \mathcal{N}_J \cup \mathcal{N}_V$, with $\Lambda(j) := \emptyset$ for $j \in \mathcal{N}_V$:

$$\left\{ \begin{array}{ll} \bar{q}_1 = \sum_{j \in \mathcal{N}_V} \bar{q}_{V,j} & j \in \mathcal{N}_J \\ \bar{q}_{l(j)} - \sum_{i \in \Lambda(j)} \bar{q}_i = 0, & j \in \mathcal{N}_J \\ \bar{q}_{l(j)} = \bar{q}_{V,j}, & j \in \mathcal{N}_V \\ \bar{h}_1(0) = \bar{h}_T & \\ \bar{h}_{l(j)}(L_{l(j)}) - \bar{h}_i(0) = 0, & i \in \Lambda(j), j \in \mathcal{N}_J \\ \bar{h}_i(L_i) - \bar{h}_i(0) + \frac{f\bar{q}_i|\bar{q}_i|}{2D_i g A_i^2} L_i = 0, & i \in \Lambda \end{array} \right. \quad (9)$$

These equations are solved for equilibrium flow \bar{q}_i and the pairs $(\bar{h}_i(L_i), \bar{h}_i(0))$, to yield the equilibrium pressure profile $\bar{h}_i(x) = \bar{h}_i(0) - \frac{f\bar{q}_i|\bar{q}_i|}{2D_i g A_i^2} x$, $x \in [0, L_i]$, for each fluid line $i \in \Lambda$. There are various algorithms for solving nonlinear equations. The Levenberg–Marquardt method is used for the subsequent simulation studies [Powell \(1968\)](#). These values are used for the feedforward (open-loop) part of the pipeline discharge valve control system.

In addition to this, a feedback controller is used to adjust the feedforward control action using sensor measurements of the end-user outlet flows. The design of this controller is based on a model obtained by linearizing about an equilibrium, as discussed next. The purpose of the feedback controller is to regulate the incremental flow (i.e., the difference between the measurements and the desired flow) at each outlet to zero. By limiting the range of frequencies up to which good feedback regulation is required, a simplified model of the infinite-dimensional linearization (which is still a PDE) can be used for controller synthesis by classical methods. The construction of such a simplified model by frequency-domain system identification is presented further in this section.

Linear incremental model

The linearized model for each fluid line $i \in \Lambda$ relates the incremental signals $\tilde{h}_i = h_i - \bar{h}_i$ and $\tilde{q}_i = q_i - \bar{q}_i$. It is obtained from (1) by first-order Taylor series approximation of the algebraic equation that specifies the relationship between flow and pressures and their partial derivatives with respect to time and space. Specifically, the linearized model takes the following form:

$$\begin{aligned} C_i \frac{\partial \tilde{h}_i}{\partial t} + \frac{\partial \tilde{q}_i}{\partial x} &= 0, \\ L_i \frac{\partial \tilde{q}_i}{\partial t} + \frac{\partial \tilde{h}_i}{\partial x} + R_i \tilde{q}_i &= 0, \end{aligned} \quad (10)$$

where

$$C_i = \frac{gA_i}{c^2}, \quad L_i = \frac{1}{gA_i}, \quad \text{and} \quad R_i = \frac{f\bar{q}_i}{gD_i A_i^2}. \quad (11)$$

The coupling conditions encode the interconnection of fluid lines as below:

$$\begin{aligned}\tilde{q}_{l(j)}(L_{l(j)}, t) - \sum_{i \in \Lambda(j)} \tilde{q}_i(0, t) &= 0, \\ \tilde{h}_{l(j)}(L_{l(j)}, t) &= \tilde{h}_i(0, t), \quad i \in \Lambda(j), \quad j \in \mathcal{N}_J.\end{aligned}\tag{12}$$

Furthermore, at the interface with the automated channel, the following hold:

$$\tilde{q}_i(0, t) = \tilde{d}_{\text{out}}(t) \quad \text{and} \quad \tilde{h}_i(0, t) = \tilde{h}_T(t), \quad i \in \Lambda(1),\tag{13}$$

where the relationship between $\tilde{d}_{\text{out}}(t) = d_{\text{out}}(t) - \sum_{j \in \mathcal{N}_V} \tilde{q}_{v,j}$ and $\tilde{h}_T(t) = h_T(t) - \bar{h}_T$ is governed by the dynamics of the automated channel, for which a linear model is detailed at the end of the next subsection.

The quality of the linear approximation can be made high by ensuring the incremental signals are sufficiently small in magnitude. The purpose of the feedback controller in the proposed approach is to keep the incremental signals small, in particular $\tilde{q}_{v,j}$, justifying the use of an incremental models for controller synthesis. In this paper, classical frequency-domain tools are considered for controller design. This involves transfer function representations of the model, as described next.

MIMO transfer function models in the frequency-domain

The relationships between the incremental pressure head and the incremental flow at the both ends of a pipe can be expressed in the form of transfer matrices. These can be derived by using the separation of variable technique to solve (10) and by applying the Laplace transform [Lin and Holbert \(2009\)](#); [Wylie \(1965\)](#). These matrices can be written in several forms which differ from each other with respect to the selected model inputs and outputs. In this work, the following admittance matrix form is used for each $i \in \Lambda$:

$$\begin{bmatrix} \tilde{Q}_i(0, s) \\ \tilde{Q}_i(L_i, s) \end{bmatrix} = \frac{1}{Z_i} \begin{bmatrix} \coth(\lambda_i(s)L_i) & -\text{csch}(\lambda_i(s)L_i) \\ \text{csch}(\lambda_i(s)L_i) & -\coth(\lambda_i(s)L_i) \end{bmatrix} \begin{bmatrix} \tilde{H}_i(0, s) \\ \tilde{H}_i(L_i, s) \end{bmatrix},\tag{14}$$

where $\text{csch}(x) = 2/(e^x - e^{-x})$, $\coth(x) = (e^x + e^{-x})/(e^x - e^{-x})$, e is Euler's number, $\lambda_i(s) = \sqrt{sC_i(sL_i + R_i)}$ is the propagation operator, with R_i, L_i, C_i as defined in (11), $Z_i = \sqrt{(sL_i + R_i)/(sC_i)}$ is the characteristic impedance, and s is the complex valued argument of the Laplace transform, which is denoted in upper case by convention; i.e., $\tilde{Q}_i(x, s) = \int_0^\infty e^{-st} q_i(x, t) dt$ denotes the Laplace transform of $q_i(x, t)$ for $s \in \{\sigma + j\omega \in \mathbb{C} \mid \int_0^\infty e^{-\sigma t} |q_i(x, t)| dt < \infty, \omega \in \mathbb{R}\}$.

The Laplace transform of the boundary conditions (12) and (13) can be collectively represented as

$$\begin{bmatrix} \tilde{H}(0, s) \\ \tilde{H}(L, s) \end{bmatrix} = \begin{bmatrix} N_u & N_d \end{bmatrix}^T \tilde{\Psi}(s),\tag{15}$$

$$\begin{bmatrix} -N_u & N_d \end{bmatrix} \begin{bmatrix} \tilde{Q}(0, s) \\ \tilde{Q}(L, s) \end{bmatrix} = \tilde{\Theta}(s),\tag{16}$$

where

$$\begin{aligned}\tilde{H}(0, s) &= \begin{bmatrix} \tilde{H}_1(0, s) \\ \vdots \\ \tilde{H}_{n_\Lambda}(0, s) \end{bmatrix}, & \tilde{H}(L, s) &= \begin{bmatrix} \tilde{H}_1(L_1, s) \\ \vdots \\ \tilde{H}_{n_\Lambda}(L_{n_\Lambda}, s) \end{bmatrix}, \\ \tilde{Q}(0, s) &= \begin{bmatrix} \tilde{Q}_1(0, s) \\ \vdots \\ \tilde{Q}_{n_\Lambda}(0, s) \end{bmatrix}, & \tilde{Q}(L, s) &= \begin{bmatrix} \tilde{Q}_1(L_1, s) \\ \vdots \\ \tilde{Q}_{n_\Lambda}(L_{n_\Lambda}, s) \end{bmatrix}, \\ \tilde{\Psi}(s) &= \begin{bmatrix} \tilde{H}_T(s) \\ \tilde{H}_V(s) \\ \tilde{H}_J(s) \end{bmatrix}, & \tilde{\Theta}(s) &= \begin{bmatrix} -\tilde{D}_{\text{out}}(s) \\ \tilde{Q}_V(s) \\ 0 \end{bmatrix},\end{aligned}$$

$\tilde{H}_V(s)$ and $\tilde{Q}_V(s)$ are column vectors of the pressure heads and flows at the valve nodes, and the matrices N_u and N_d are upstream and downstream link-node incidence matrices, as described further in [Zecchin et al. \(2009\)](#). It now follows from (14) that

$$\begin{aligned}\tilde{\Theta}(s) &= \begin{bmatrix} -\tilde{D}_{\text{out}}(s) \\ \tilde{Q}_V(s) \\ 0 \end{bmatrix} = \begin{bmatrix} \mathbf{Y}_{TT}(s) & \mathbf{Y}_{TV}(s) & \mathbf{Y}_{TJ} \\ \mathbf{Y}_{VT}(s) & \mathbf{Y}_{VV}(s) & \mathbf{Y}_{VJ} \\ \mathbf{Y}_{JT}(s) & \mathbf{Y}_{JV}(s) & \mathbf{Y}_{JJ} \end{bmatrix} \begin{bmatrix} \tilde{H}_T(s) \\ \tilde{H}_V(s) \\ \tilde{H}_J(s) \end{bmatrix} \\ &= \mathbf{Y}(s)\tilde{\Psi}(s),\end{aligned}\tag{17}$$

where

$$\mathbf{Y}(s) = \begin{bmatrix} -N_u & N_d \end{bmatrix} \begin{bmatrix} \text{diag}(\mu_i(s)) & \text{diag}(-\nu_i(s)) \\ \text{diag}(\nu_i(s)) & \text{diag}(-\mu_i(s)) \end{bmatrix} \begin{bmatrix} N_u & N_d \end{bmatrix}^T,\tag{18}$$

with $\mu_i(s) = \frac{1}{Z_i} \coth(\lambda_i(s)L_i)$ and $\nu_i(s) = \frac{1}{Z_i} \text{csch}(\lambda_i(s)L_i)$, $i \in \Lambda$.

Resolving the vector of internal junction pressures, $\tilde{H}_V(s)$, yields the following model relating on the signals that are relevant to the interface with the automated supply channel and feedback control design for the pipeline network discharge valves:

$$\begin{bmatrix} -\tilde{D}_{\text{out}}(s) \\ \tilde{Q}_V(s) \end{bmatrix} = \begin{bmatrix} \mathbf{G}_{TT}(s) & \mathbf{G}_{TV}(s) \\ \mathbf{G}_{VT}(s) & \mathbf{G}_{VV}(s) \end{bmatrix} \begin{bmatrix} \tilde{H}_T(s) \\ \tilde{H}_V(s) \end{bmatrix},\tag{19}$$

where

$$\begin{bmatrix} \mathbf{G}_{TT} & \mathbf{G}_{TV} \\ \mathbf{G}_{VT} & \mathbf{G}_{VV} \end{bmatrix} = \begin{bmatrix} \mathbf{Y}_{TT} & \mathbf{Y}_{TV} \\ \mathbf{Y}_{VT} & \mathbf{Y}_{VV} \end{bmatrix} - \begin{bmatrix} \mathbf{Y}_{TJ} \\ \mathbf{Y}_{VJ} \end{bmatrix} \mathbf{Y}_{JJ}^{-1} \begin{bmatrix} \mathbf{Y}_{JT} & \mathbf{Y}_{JV} \end{bmatrix}.\tag{20}$$

Now also resolving the relationship $\tilde{H}_T(s) = T(s)\tilde{D}_{\text{out}}$, which corresponds to the dynamic response of the automated supply channel to variation in the downstream flow load, results in the transfer function model that relates the discharge valve flows and corresponding local pressure heads:

$$\begin{aligned}\tilde{Q}_V(s) &= \left(\mathbf{G}_{VV}(s) - \mathbf{G}_{VT}(s)T(s)(I + \mathbf{G}_{TT}(s)T(s))^{-1}\mathbf{G}_{TV}(s) \right) \tilde{H}_V(s) \\ &= \mathbf{G}(s)\tilde{H}_V(s).\end{aligned}\tag{21}$$

Taking the Laplace transform of (5), whereby $\widetilde{H}_T(s) = \frac{1}{s}(c_{in}e^{-s\tau}\widetilde{Q}_{in}(s) - c_{out}(\widetilde{Q}_{out}(s) + \widetilde{D}_{out}(s)))$, it follows that for given channel feedback controller $\widetilde{Q}_{in}(s) = -C(s)\widetilde{H}_T(s)$,

$$T(s) = -\frac{c_{out}}{(s + c_{in}e^{-s\tau}C(s))}. \quad (22)$$

In subsequent sections the channel controller is taken to be of the form

$$C(s) = \frac{K_d(T_I s + 1)}{T_I s(T_F s + 1)}; \quad (23)$$

i.e., a proportional plus integral controller with additional lag for steeper roll-off at high-frequency. Such controllers are used in practice; e.g., see [Cantoni et al. \(2007\)](#). The control design for irrigation channels in a demand-driven configuration is also discussed in [Litrice and Fromion \(2004\)](#); [Litrice et al. \(2007\)](#); [Cantoni and Mareels \(2020\)](#). The transfer function matrix $G(s)$ is irrational. To enable application of classical feedback controller synthesis tools, a method for constructing a suitable rational approximation is described next.

Reduced order approximation

The transfer function matrix $G(s)$ in (21) relating the vector of incremental valve openings $\widetilde{U}_V(s)$ to the incremental flows $\widetilde{Q}_V(s)$ is an irrational function of s . A rational approximation is required to enable application of the \mathcal{H}_∞ loopshaping based procedure for centralized feedback controller synthesis considered in the next section. The approximation approach followed here involves the application of a standard system identification method to match frequency-response samples generated from the irrational transfer function model to those of a lower order rational transfer function model [Pintelon and Schoukens \(2012\)](#). This is done element-wise as detailed below.

Given element $G_{ij}(s)$ on row i and column j of $G(s)$, a rational approximation $\hat{G}_{ij}(s) = a_{ij}(s)/b_{ij}(s)$, in which $a_{ij}(s) = \sum_{k=0}^{m_{ij}} \alpha_k s^k$ and $b_{ij}(s) = \sum_{k=0}^{m_{ij}} \beta_k s^k$ are polynomials of given degree m_{ij} with $\beta_{m_{ij}} \neq 0$, is obtained by solving an least-squares optimization problem

$$\min_{\substack{\alpha_0, \dots, \alpha_{m_{ij}} \\ \beta_0, \dots, \beta_{m_{ij}}}} \sum_{n=1}^N |W(j\omega_n)(G_{ij}(j\omega_n) - \hat{G}_{ij}(j\omega_n))|^2 \quad (24)$$

$$\text{subject to } \hat{G}_{ij} \text{ has no pole with non-negative real part,} \quad (25)$$

for a set of sample frequencies $\{\omega_n\}_{n=1}^N$ and weight $W(s)$. In this work, the sample frequencies are selected to ensure good matching at low frequencies, under the premise that the feedback controller to be designed will roll-off at high frequency (providing robustness to high-frequency modelling error), and the weight is taken to be $W(s) = 1/G_{ij}(s)$ so that the measure of error is relative. The resulting optimization problem is solved using the 'tfest' function [Ozdemir and Gumussoy \(2017\)](#) from the MATLAB system identification toolbox. An alternative approach is to identify the entire transfer matrix of the MIMO system simultaneously, which might be advantageous if there is a large number of valves. However, the element-wise approach led to a lower-order model in the example presented in the case study.

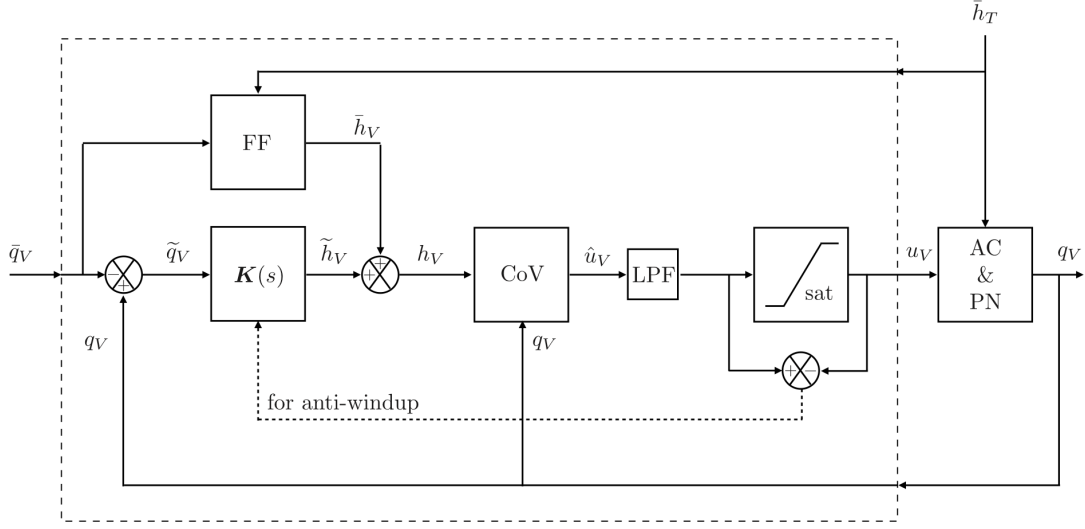


Fig. 2. Discharge valve control system block diagram. The controller consists of a feedforward component (FF) and a feedback compensator $K(s)$. The block labelled AC & PN represents the dynamics of the pipeline network (PN) coupled to the automated channel (AC). The static non-linear change-of-variables (CoV) is defined in (26).

DISCHARGE VALVE CONTROL SYSTEM DESIGN

The architecture of the proposed control system is shown in Figure 2, in the form that is ultimately simulated for a full non-linear distributed parameter model of the automated channel and pipeline dynamics in the block denoted by AC & PN. It can be seen that the control system comprises two parts; the feedforward controller denoted by FF, and feedback controller with transfer function $K(s)$. The goal of the feedback controller is to bring the discharge flows q_V to desired reference values, by dynamically compensating for observed error in the response to the purely model-based feedforward control action. The feedforward controller solves (9) to yield the steady-state valve pressure heads $\bar{h}_{V,j} = \bar{h}_{l(j)}(L_{l(j)})$, $j \in \mathcal{N}_V$, for given desired discharge flow $\bar{q}_{V,j}$, $j \in \mathcal{N}_V$, and supply-channel water level set-point \bar{h}_T .

The feedback controller determines $\tilde{h}_{V,j}$, the incremental pressure for each valve $j \in \mathcal{N}_V$, in response to observed incremental flow signal $\tilde{q}_{V,j} = q_{V,j} - \bar{q}_{V,j}$, where $q_{V,j}$ is the measured flow at valve $j \in \mathcal{N}_V$ (i.e., in response to the error between measured and desired flow.) These incremental pressures are added to the feedforward steady-state pressures $\bar{h}_{V,j}$. The sum is translated to corresponding valve openings via the following static non-linear change-of-variables (denoted by CoV in Figure 2):

$$\hat{u}_{V,j} = \begin{cases} q_{V,j} / (\gamma_j \sqrt{2 \cdot g \cdot h_{V,j}}), & h_{V,j} > 0 \\ u_{V,j}^{max}, & h_{V,j} \leq 0 \end{cases} \quad (26)$$

where $h_{V,j} = \bar{h}_{V,j} + \widetilde{h}_{V,j}$ for $j \in \mathcal{N}_V$ is the output of the controller, not the actual valve head. This non-linear compensation enables the use of a linearized model for feedback controller design, as discussed further below.

The feedback controller transfer function $\mathbf{K}(s)$ is designed using the linearized dynamics for a suitably chosen steady-state operating point. Both decentralized and centralized feedback control are considered. The decentralized case corresponds to a diagonal transfer function matrix $\mathbf{K}(s)$, with each component $K_{ii}(s)$ designed using classical loop-shaping ideas, with only indirect regard for the coupling between outlets by respecting limits on the control loop bandwidth. With a view to understanding the potential for improved performance, the centralized controller is designed via the \mathcal{H}_∞ loop-shaping method, based these decentralized compensators $K_{ii}(s)$ as weights, and the rational approximation $\hat{\mathbf{G}}(s)$ of the linear model $\mathbf{G}(s)$ in (21), for a suitable operating point. The selection of this operating point and design of the decentralized compensators are elaborated within the context of the case study. The form of the decentralized compensator and the \mathcal{H}_∞ loopshaping synthesis method are described in the next two subsections.

To account for the typical stroking limits of the valve, and to also limit interactions that can arise from water-hammer, the valve opening command \hat{u}_V is low-pass filtered, by the block denoted by LPF in Figure 2, to remove high frequency components of the command (e.g., arising from step change of the feedforward control action.) The corresponding diagonal transfer matrix L has non-zero entries of the form

$$L_{ii}(s) = \frac{\omega_{0,i}}{s + \omega_{0,i}}, \quad (27)$$

where $\omega_{0,i}$ are the filter cutoff frequencies. In the design of the decentralized compensators, the presence of this filter is accounted indirectly by limiting the control loop bandwidth according. The saturation block in the path to the valve opening u_V enables detection of valve position saturation for the purpose of anti-windup compensation in the controller implementation [Astrom and Rundqwist \(1989\)](#). Such compensation is required because the feedback controller $\mathbf{K}(s)$ will include integral action. This integral action robustly ensures zero error (i.e., $\widetilde{q}_V = 0$) in the steady-state response to step changes in the discharge flow demand, provided the closed-loop is stable [Goodwin et al. \(2001\)](#).

Form of the decentralized feedback compensators

The decentralized controller is designed using classical loop-shaping ideas. For introductions to these ideas see [Åström and Murray \(2010\)](#); [Skogestad and Postlethwaite \(2007\)](#), for example. Each diagonal entry of the decentralized controller takes the form of a PI (Proportional-Integral) compensator:

$$\mathbf{K}_{ii}(s) = -\frac{k_{p,i}s + k_{int,i}}{s \cdot (k_{f,i}s + 1)}. \quad (28)$$

This can be realized with the state-space equations

$$\begin{aligned}\dot{x}_{f,i} &= -\frac{1}{k_{f,i}}x_{f,i} + \frac{1}{k_{f,i}}\tilde{q}_{V,i} \\ \dot{x}_{\text{int},i} &= x_{f,i} \\ \tilde{h}_{V,i} &= -k_{p,i}x_{f,i} - k_{\text{int},i}x_{\text{int},i}.\end{aligned}\tag{29}$$

The parameters $k_{p,i}$ are the proportional gains of the decentralized compensators, $k_{\text{int},i}$ the integral gains, and $k_{f,i}$ the roll-off filter time-constants.

The values of these gains are tuned to achieve the desired feedback control performance. For the problem at hand, the main objective is to robustly achieve $\tilde{q}_V = 0$ in steady-state, with acceptable transients in response to step disturbances associated with changes in operating point. The integral action in (29) ensures $\tilde{q}_V = 0$ in steady-state provided the closed-loop is stable. Increasing the value of the proportional gain k_p tends to increase the speed of the response when perturbed from steady-state. The integral gain k_{int} is set to limit the range of low frequencies over which the PI compensator introduces significant phase lag to the control loop. In conjunction with large proportional gain this phase lag can lead to undesirable oscillations in the transient response. The proportional gain parameter is also constrained by the requirement that the compensated loop cross-over frequency, beyond which the loop gain is less than 1, be limited in line with the aforementioned low-pass filter at the control valves, which also filters the feed-forward control action. The choice of parameters is guided by the corresponding diagonal block $\mathbf{G}_{ii}(s)$ of the network dynamics, with only indirect consideration of coupling between the outlets. Limits on the proportional gain also provide robustness to high-frequency model uncertainty of the kind associated with neglecting the coupling, and the approximate rational model $\hat{\mathbf{G}}(s)$ of the distributed-parameter model $\mathbf{G}(s)$, which is subsequently used for centralized controller synthesis. The roll-off filter parameter $k_{f,i}$ in (28) further limits the control loop gain at high frequencies for promoting such robustness. The selection of compensator parameters is discussed further within the context of the case studies.

As there are physical limits $0 \leq u_{v,i}(t) \leq u_{v,i,\text{max}}$ on the control valve openings and integral action in the feedback controller $\mathbf{K}(s)$, an anti-windup strategy must be implemented [Astrom and Rundqwist \(1989\)](#). Integral windup occurs when the integral terms of the controller accumulate a significant error as a result of saturated actuators when the desired output is not achievable. The accumulated integral error without anti-windup compensation can lead to large overshoots and undesirable transients in response to changes/disturbances. In the case studies that follow, a simple clamping anti-windup strategy, such that the state $x_{\text{int},i}$ corresponding to the integrator in the implementation (29) of $\mathbf{K}_{ii}(s)$, remains fixed at the value saturation occurs until the value is no longer in saturation; i.e., the right-hand side of (29) is made zero during saturation.

H_∞ loop-shaping synthesis

With a view to more directly accounting for the coupling between the outlets, the decentralized controller is augmented via the so-called \mathcal{H}_∞ loop-shaping synthesis

Parameter	SI unit	Value
c - wave speed in the water	m/s	1200
g - gravity acceleration	m/s ²	9.81
f - friction coefficient		0.016
D - pipe diameter	m	$D_1, D_2, \dots, D_5 = 0.634$
L_p - pipe length	m	$L_1 = 500; L_2, L_4 = 300;$ $L_3 = 800; L_5 = 700$
γ - coefficient of discharge		$\gamma = 0.7$

TABLE 1. Simulation parameters.

c_{in}	c_{out}	τ (min)	K_d	T_I (min)	T_F (min)
0.0174	0.0174	12	0.638	146.78	17.366

TABLE 2. System identification model parameters and the controller parameters for the irrigation channel.

method of [McFarlane and Glover \(1990, 1992\)](#). The approach involves use the MIMO system model $\hat{G}(s)$, a pre-compensator $W_1(s)$, and a post-compensator $W_2(s)$, which form the shaped open-loop

$$G_s(s) = W_2(s)\hat{G}(s)W_1(s). \quad (30)$$

Guidance on the design of the weights $W_1(s)$ and $W_2(s)$ in standard control contexts can be found in [Hyde and Glover \(1993\)](#); [Skogestad and Postlethwaite \(2007\)](#). In this work, the pre-compensator $W_1(s)$ is taken to be the diagonal transfer function with non-zero entries set to the transfer functions $K_{ii}(s)$ of the decentralized controller, and $W_2(s)$ is set to the identity matrix.

A stabilizing MIMO feedback controller $K_s(s)$ is synthesized for the shaped open-loop transfer function $G_s(s)$ to minimize the \mathcal{H}_∞ norm of the block 2×2 transfer function matrix comprising the ‘gang-of-four’ (in the language of [Åström and Murray \(2010\)](#)) closed-loop sensitivity transfer matrices. The \mathcal{H}_∞ norm is the supremum of the largest singular value of the transfer matrix over all frequencies, and consideration of the ‘gang-of-four’ transfer functions has important performance and robustness interpretations [McFarlane and Glover \(1990, 1992\)](#); [Skogestad and Postlethwaite \(2007\)](#). The required synthesis procedure is available as the function `ncfsyn` in the robust control toolbox of MATLAB [Glover and McFarlane \(1992\)](#); [McFarlane and Glover \(1990\)](#). The feedback controller $W_1(s)K_s(s)W_2(s)$ is implemented. This centralized controller is denoted by $K_\infty(s)$ subsequently to distinguish it from the decentralized feedback controller $K(s) = W_1(s)$ described above. Note that $K_\infty(s)$ is the MIMO augmentation $K_s(s)$ of the decentralized controller $K(s)$.

CASE STUDY

The water distribution system shown schematically in Figure 1 is considered for testing in simulation the developed approaches to pipeline network control. The system consists of a network of five pipelines and three control valves at the outlets. The parameters of the system used in these simulations are given in Table 1, and the parameters of the channel that supplies the water to the pipeline system are given in Table 2. These parameters have been motivated by a prototype pipeline network installed in the Goulburn Murray irrigation district in Victoria, Australia. The network geometry and valve locations have been determined based on the location of the existing supply channel and the fields that are to be irrigated. The tank head is sufficient to provide a flow rate of approximately 10 megaliters per day to each valve under the power of gravity. Moreover, a pump is installed at the pipeline inlet, which is inactive most of the time but can be used to boost the water head if higher flows are required. The valves are equipped with flow meters and the valve openings are the control inputs that are determined by the controller as outlined in Figure 2.

Linearized transfer matrices and model reduction

The transfer functions of the pipeline system are determined from (21) by linearizing the system around multiple equilibrium points, considering a range of output flows. Plots of the transfer functions for two chosen flow rates are given in Figure 3. The first model is generated by use of $\bar{Q}_{v,1} = \bar{Q}_{v,2} = \bar{Q}_{v,3} = 0.10 \text{ m}^3/\text{s}$ (linear model \mathbf{G}_1) and the second one using $\bar{Q}_{v,1} = \bar{Q}_{v,2} = \bar{Q}_{v,3} = 0.05 \text{ m}^3/\text{s}$ (linear model \mathbf{G}_2). The reference water level of the irrigation channel is fixed at $\bar{h}_T = 1.5 \text{ m}$ for the both cases. The remaining parameters of the linearized model are found by solving the steady-state equations (9) by use of the Levenberg-Marquardt method, using a zero initial guess for the numerical solver. The steady state solution for the pressure head at the valve opening of the linearized model \mathbf{G}_1 are $\bar{H}_{v,1} = 0.88 \text{ m}$, $\bar{H}_{v,2} = 0.47 \text{ m}$ and $\bar{H}_{v,3} = 0.42 \text{ m}$, and for the linearized model \mathbf{G}_2 are $\bar{H}_{v,1} = 1.34 \text{ m}$, $\bar{H}_{v,2} = 1.24 \text{ m}$ and $\bar{H}_{v,3} = 1.29 \text{ m}$.

In Figure 3, one can see that the pipeline network is close to steady state for flows varying with a frequency of up to $5 \cdot 10^{-3} \text{ rad/s}$. The slight bumps at around $2 \cdot 10^{-4} \text{ rad/s}$ are due to the response of the supplying channel. While close to a static steady-state (i.e., low frequency), the diagonal entries of \mathbf{G} have 180 degree phase, indicating that lower pressure corresponds to higher flow. This agrees with intuition, as a higher flow increases the pressure loss between tank and valve due to friction, resulting in a lower valve pressure. Whereas the off-diagonal entries have zero phase, indicating that higher pressure at one valve increases flow through the other valves. The magnitudes at low frequencies correspond to the frictional head loss through the valve, with the difference between the linearizations around the two flow rates also being due to differences in the steady-state frictional head loss. The frequency responses then roll off with higher frequencies until the resonances start at around 2 rad/s . Some of the resonant magnitude peaks exceed the respective steady state gains.

Feedback controller design

In order to attenuate the resonances starting at approximately 2 rad/s , the cut-off frequency of the low-pass filter \mathbf{L} after the change of variable in Figure 2 is chosen to be $\omega_0 = 0.2 \text{ rad/s}$; see, (27). This filter can also be set to take into account actuator

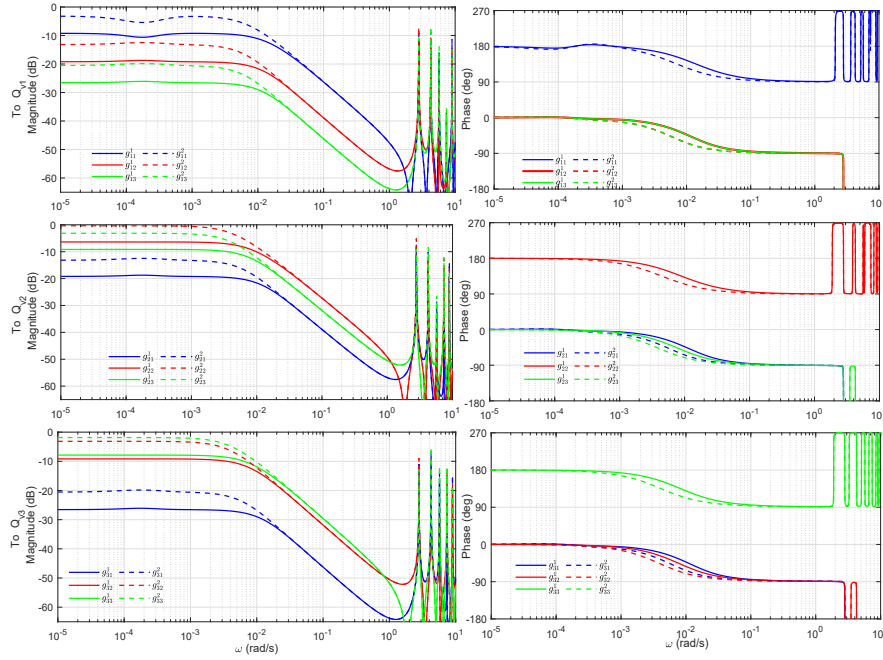


Fig. 3. Plots of the transfer functions in $\mathbf{G}(s)$ derived around the reference flows: $\bar{Q}_{v,1} = \bar{Q}_{v,2} = \bar{Q}_{v,3} = 0.10 \text{ m}^3/\text{s}$ (entries g_{ij}^1 , $i, j = 1, 2, 3$) and $\bar{Q}_{v,1} = \bar{Q}_{v,2} = \bar{Q}_{v,3} = 0.05 \text{ m}^3/\text{s}$ (entries g_{ij}^2).

limitations. For instance, if there is a limit on the rate at which the physical valve can open, the low-pass filter can be made so slow that the actual valve opening is able to follow the signal.

The parameters of the i -th diagonal entry of the decentralized controller $\mathbf{K}(s)$ in (28) are selected as $k_{p,i} = 5$, $k_{\text{int},i} = 0.02$ and $k_{f,i} = 50$ for all three valves $i = 1, 2, 3$. The compensator rolls-off time-constant $k_{f,i}$ is chosen one hundred fold slower than that of the pole of the low-pass filter \mathbf{L} in the faster inner change-of-variables loop. This averts undesirable interactions between the two loops by separation of time scales [Kokotović et al. \(1999\)](#). It also ensures low control-loop gain at high frequencies, where the error associated with subsequently using $\hat{\mathbf{G}}(s)$ for centralized controller synthesis as a model becomes significant.

The correspondingly compensated open-loop $\mathbf{G}(s)\mathbf{K}(s)$ is shown in Figure 4. Note that the cross-over frequency for each diagonal component of around 0.02 rad/s for the model $\mathbf{G}_2(s)$ (i.e., operating point 0.05 m³/s.) This is about two decades below the resonances, and also a decade below the cut-off frequency ω_0 of the filter \mathbf{L} in the inner CoV-loop. The model $\mathbf{G}_2(s)$ is considered to inform the control design because the corresponding resonances are less damped due to the smaller friction losses at the lower flow rate.

For synthesis of the centralized controller by \mathcal{H}_∞ loop-shaping, the rational transfer function $\hat{\mathbf{G}}$ is generated using the reduced order approximation previously presented. The reduced model is optimized to match the original model in the frequency range of

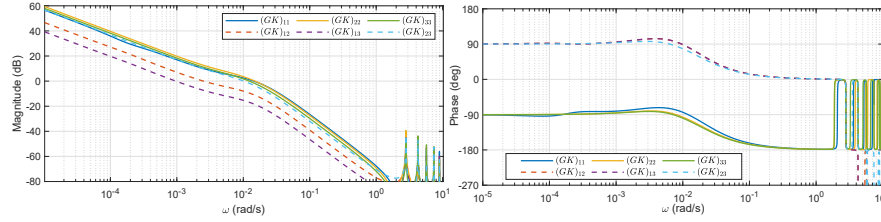


Fig. 4. The Bode plot of the compensated open-loop GK with decentralized controller with entries $K_{ii}(s)$ as in (28). Only half of the off-diagonal entries are shown due to symmetry.

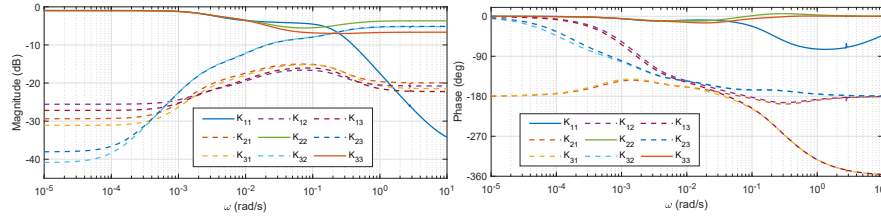


Fig. 5. Bode plot of the controller K_s synthesized by the \mathcal{H}_∞ procedure. The solid lines show the diagonal entries and the dashed lines show the off-diagonal entries.

$\omega \in [0 : 3]$ rad/s and each entry of the 3×3 transfer matrix G is estimated with a 3-rd order model. A good match match of the two models in the desired frequency range is achieved with Normalized Root-Mean Square Error (NRMSE) fit of 94 – 98 %.

Synthesis of the centralized feedback controller $K_\infty(s) = K_s(s)K(s)$ is carried out as described in the previous section. Bode plots of the MIMO compensator $K_s(s)$ are given in Figure 5. At low frequencies, it is diagonal-dominant, i.e., very similar to a decentralized one. The DC gain is slightly smaller than 1. At higher frequencies, at around cross-over, the off-diagonal components of K_s become more significant.

A reduced-order approximation of the controller K is generated for use in the simulations using implicit balancing techniques [Varga \(1991\)](#), resulting in a 5 – th order linear time invariant system from the initially large 29 – th order controller. The reduced-order and the original controller are nearly identical beyond the cross-over frequency of around 0.02 rad/s that can be seen in the singular value plots in Figure 6.

Simulation results

The simulations are performed using numerical implementation of the model in the MATLAB Simulink environment. The simulation model of the water hammer PDEs (1) is developed using implicit nonlinear finite-difference model presented in [Scola et al. \(2018\)](#).

Four different implementations are considered for both the decentralized and centralized controllers:

1. pure feedback control without feed-forward;
2. pure feed-forward without feedback control;

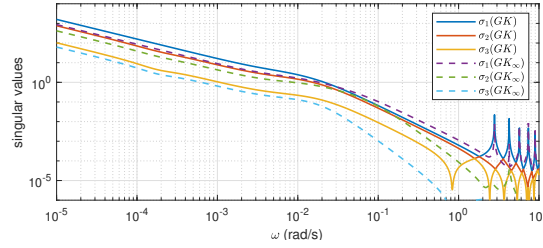


Fig. 6. Singular values of the compensated open-loop with decentralized and centralized controllers.

3. feedback control with feed-forward, where (9) is computed based on the water-level set-point in the tank, which only requires global “event-triggered” communication of the changes; and
4. feedback control with feed-forward, where (9) is updated continuously based on the measured channel water level.

The communication overhead varies significantly between these implementations. Pure decentralized feedback without feed-forward uses only local measurements at each valve, i.e., no global communication is required. For centralized control, continuous communication between a central host and all valves is required. If the feed-forward is based on set-point values of the channel water-level and discharge flow demand, then only change event-driven communication is required to determine the feed-forward control action. The continuously updated feed-forward requires communication of the channel water-level measurements to all valves at all times.

The control performance is tested around different operation points by varying the desired flow in the range of $0.05 - 0.1 \text{ m}^3/\text{s}$, which lies within the range of the feasible flows that are set by the reference pressure delivered by the channel and the limited ranges of the valve openings. In these simulations the feed-forward signal is generated based on a model with 10% error in the friction term for each pipeline.

The performance of the different control schemes are compared in Figure 7, for implementations 1 and 2, and Figure 8 for implementation 3 and 4. In the case where only feed-forward control is used, the error in friction leads to significant steady-state error. The variations in the water level in the channel causes additional slow (over the course of hours) fluctuations in the valve flows if the feed-forward is only updated when there is a change in the reference flow. The plots of the evolution of the valve pressure heads and openings for the implementation 4 are given in Figure 9.

For the schemes involving feedback control, the integral action robustly brings the valve flows to the demand set-point in steady state. Desired performance, including transient response, is observed for a broad ranges of operating points. Thus, for the operating range considered, there is no apparent need to schedule different controllers. There is also no clear value in continuous update of the feedforward control based on channel water-level measurements. The performance of all shown feedback control schemes is comparable, which suggests the decentralized feedback with event-driven

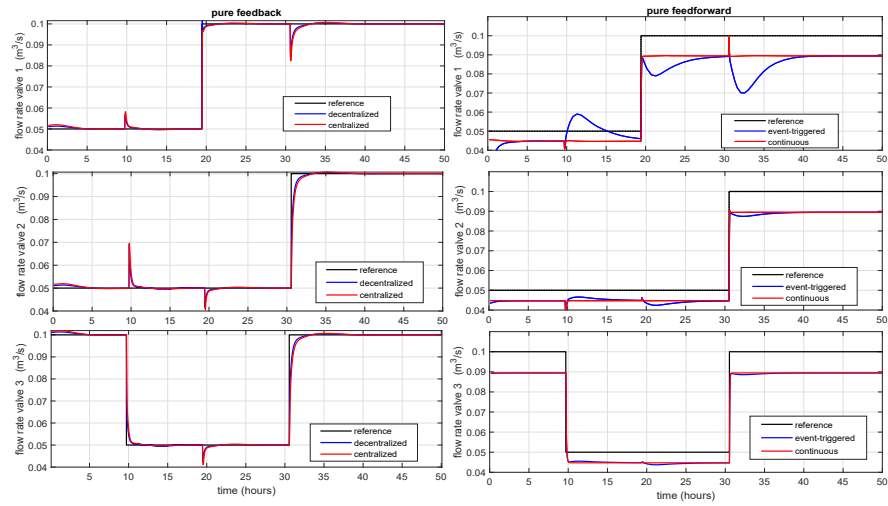


Fig. 7. Plots of the valve flows using pure feedback control (left) and pure feed-forward (right).

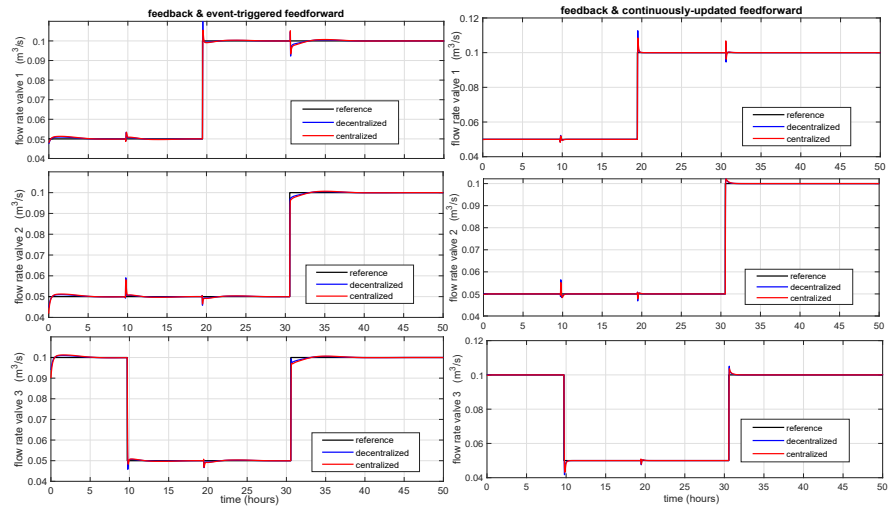


Fig. 8. Plots of the valve flows using both feedback and feedforward control where the feed-forward signal is computed based on the reference (left) and actual (right) water level in the supply channel.

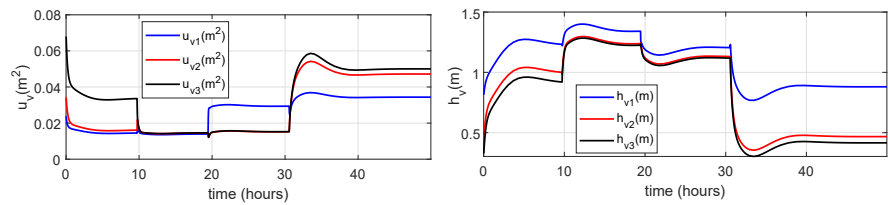


Fig. 9. Plots of the valve pressure heads and the openings when using combination of feedback and feedforward control, where the feed-forward signal is computed based on the actual water level in the supply channel.

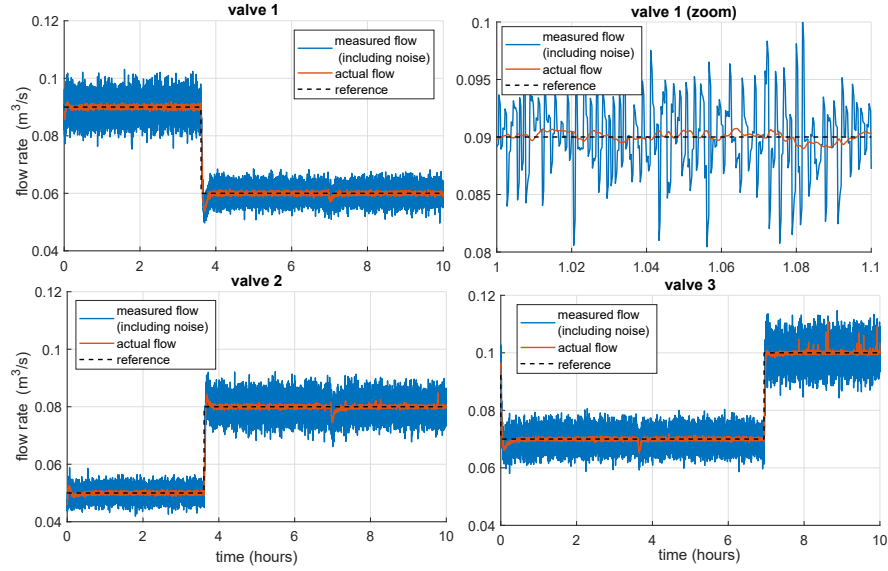


Fig. 10. Plots of the valve flows with measurement noise.

feedforward would be most suitable for this network in light of the significantly lower communication overhead.

The dynamic coupling between the valves is clearly visible in Figures 7 and 8. For instance, in the left column of Figure 7, the drop in flow through valve 3 at time 10 hours causes a spike in the flows through valves 1 and 2. This is similar to the transfer functions \mathbf{G} in Figure 3 (note that \mathbf{G} were open-loop transfer functions whereas the simulations show the response of the controlled closed-loop system), in that a reduction in flow 3 corresponds to a pressure increase at valve 3, which causes a flow increase at the other valves. After a brief transient spike, the feedback controller compensates and the flows return to reference. In the simulations with feedforward in Figure 8, the coupling is still visible but less significant because the feedforward term pre-emptively adjusts the other valve openings.

The attenuation of high-frequency measurement noise is investigated in Figure 10, at the example of the feedback controller with feed-forward that is only updated when there are changes in the reference flow. The noise signal is constructed by passing a random white noise signal through a high-pass filter with frequency response $\frac{s}{\omega_{hp} + s}$ with $\omega_{hp} = 0.2$ rad/s. The noise signal is assumed proportional to the actual flow and is scaled such that the noise amplitude amount to approximately 10% of the actual flow. As shown in Figure 10, the feedback control scheme and, in particular the low-pass filter in the inner loop adjusting the valve opening (see Figure 2) effectively dampens the effect that the noise has on the actual valve flows. The sensitivity with respect to measurement noise depends on the frequency range of the noise, as determined by the parameter ω_{hp} . In general, higher frequency noise is dampened more effectively by the low-pass filter, whereas lower-frequency noise can be compensated by reducing ω_0 in (27) if required.

The difference in performance between the centralized and decentralized controllers tends to become more significant if performance is pushed further, e.g., if the crossover frequency is designed close to the first resonance. Whether performance should be pushed that much depends on considerations such as practical performance requirements and actuator limits. For instance, in extremely long pipelines, the resonant frequencies are lower and might get closer to the frequency range over which flow tracking is required, although in long pipes friction also tends to weaken the coupling between the valves. The framework for modelling and control developed in this paper nonetheless provides scope for exploring exploration of design trade-offs as in the case study presented.

CONCLUSION AND FUTURE WORK

In this work a control-oriented model of irrigation-channel supplied pipeline networks is developed and used to devise automatic controllers for regulating discharge flows to specified demand. The model is developed by linearizing continuity and momentum equations and determining the transfer functions which capture coupling from each controlled input of the system to each output. The presented modeling framework permits quantitative examination of the whole network and the coupling between all individual discharge outlets and the supply channel. These models are straightforward to be use for control design. In principle, a wide variety of different feedback control methods can be considered on the basis of such models.

Compensating the nonlinearity of the valve equation via a change-of-variables, enables the design of a single linear feedback controller that can be used for a range of operating points (flow demands). In the case when the nonlinear nature of the system is more significant due to an even wider range of flows, it is possible to extract different models around multiple operation points and schedule the controllers [Rugh and Shamma \(2000\)](#).

Different control configurations using decentralized and centralized feedback control have been compared. The decentralized controller with no feedforward, which requires no information exchange between the valves or the supplying channel, achieves satisfactory tracking of reference flows. The centralized controller based on the model of the coupling between the valves yield modest improvement in performance, at the cost of substantially higher communication overhead. The addition of feedforward based on the static nonlinear model and set-point change driven update at low communication and computation overhead, improves performance significantly for both centralized and decentralized controllers.

The structure of the control models could significantly increase in order when the approaches is used for a large number of pipelines and control valves. This would raise the complexity of the centralized controller synthesis method. In such situations, and if performance of the fully decentralized controller is not sufficient, it could be worth to investigate the possibility of applying partly decentralized control in parts of the network where the coupling is weak.

The models used in this works are developed for pressurized flow pipeline networks. In future work these models can be extended by considering the case when the

pipelines are not fully pressurized. For this aim the models could be modified using models for transient-mixed flows [Bouso et al. \(2012\)](#).

DATA AVAILABILITY STATEMENT

All data, models, or code that support the findings of this study are available from the corresponding author upon reasonable request.

ACKNOWLEDGMENTS

This work was supported in part by and Rubicon Water Pty. Ltd., and the Australian Research Council (LP160100666).

REFERENCES

- Åström, K. J. and Murray, R. M. (2010). *Feedback systems: an introduction for scientists and engineers*. Princeton university press.
- Astrom, K. J. and Rundqwist, L. (1989). “Integrator windup and how to avoid it.” *1989 American Control Conference*, IEEE, 1693–1698.
- Bartecki, K. (2016). “Transfer function models for distributed parameter systems: Application in pipeline diagnosis.” *IEEE Conference on Control and Fault-Tolerant Systems (SysTol)*, IEEE, 145–151.
- Bermúdez, J. R., López-Estrada, F. R., Besançon, G., Valencia-Palomo, G., and Martínez-García, C. (2021a). “Optimal control in a pipeline coupled to a pressure reducing valve for pressure management and leakage reduction.” *SysTol 2021 - 5th International Conference on Control and Fault-Tolerant Systems*, Saint-Raphaël, France.
- Bermúdez, J. R., Martínez-García, C., López-Estrada, F. R., Besançon, G., and Valencia-Palomo, G. (2021b). “Pressure management to reduce leaks in water distribution systems by means of a pressure reducing valve.” *Memorias del Congreso Nacional de Control Automático*, Guanajuato, Mexico.
- Bouso, S., Daynou, M., and Fuamba, M. (2012). “Numerical modeling of mixed flows in storm water systems: critical review of literature.” *Journal of Hydraulic Engineering*, 139(4), 385–396.
- Cantoni, M. and Mareels, I. (2020). *Demand-Driven Automatic Control of Irrigation Channels*. Springer London, London, 1–10.
- Cantoni, M., Weyer, E., Li, Y., Ooi, S. K., Mareels, I., and Ryan, M. (2007). “Control of large-scale irrigation networks.” *Proceedings of the IEEE*, 95(1), 75–91.
- Chaudhry, M. H. (1979). *Applied hydraulic transients*. Springer.
- Chaudhry, M. H. (2007). *Open-channel flow*. Springer Science & Business Media.

- Dai, P. D. (2021). “Optimal pressure management in water distribution systems using an accurate pressure reducing valve model based complementarity constraints.” *Water*, 13(6), 825.
- De Persis, C. and Kallesoe, C. S. (2011). “Pressure regulation in nonlinear hydraulic networks by positive and quantized controls.” *IEEE Transactions on Control Systems Technology*, 19(6), 1371–1383.
- Fox, J. (1977). *Hydraulic analysis of unsteady flow in pipe networks*. A Halsted Press book. Halsted Press.
- Galuppini, G., Creaco, E., and Magni, L. (2020). “A gain scheduling approach to improve pressure control in water distribution networks.” *Control Engineering Practice*, 103, 104612.
- Glover, K. and McFarlane, D. (1992). “A loop shaping design procedure using H_∞ synthesis.” *IEEE Transactions on Automatic Control*, 37(6), 759–769.
- Goodwin, G. C., Graebe, S. F., Salgado, M. E., et al. (2001). *Control system design*, Vol. 240. Prentice hall New Jersey.
- Hyde, R. A. and Glover, K. (1993). “The application of scheduled H_∞ controllers to a vstol aircraft.” *IEEE Transactions on Automatic Control*, 38(7), 1021–1039.
- Kaltenbacher, S., Steffelbauer, D. B., Cattani, M., Horn, M., Fuchs-Hanusch, D., and Römer, K. (2017). “A dynamic model for smart water distribution networks.” *CCWI2017: Computing and Control for the Water Industry*.
- Kaltenbacher, S., Steinberger, M., and Horn, M. (2018). “Modeling hydraulic networks for control: How to deal with consumption?.” *IEEE control systems letters*, 2(4), 671–676.
- Kim, S. H. (2008). “Address-oriented impedance matrix method for generic calibration of heterogeneous pipe network systems.” *Journal of Hydraulic Engineering*, 134(1), 66–75.
- Koech, R. and Langat, P. (2018). “Improving irrigation water use efficiency: A review of advances, challenges and opportunities in the Australian context.” *Water*, 10(12), 1771.
- Kokotović, P., Khalil, H. K., and O’reilly, J. (1999). *Singular perturbation methods in control: analysis and design*. SIAM.
- Lin, K. and Holbert, K. E. (2009). “Applying the equivalent PI circuit to the modeling of hydraulic pressurized lines.” *Mathematics and Computers in Simulation*, 79(7), 2064 – 2075.
- Litrico, X. and Fromion, V. (2004). “Simplified modeling of irrigation canals for controller design.” *Journal of irrigation and drainage engineering*, 130(5), 373–383.

- Litrico, X., Malaterre, P.-O., Baume, J.-P., Vion, P.-Y., and Ribot-Bruno, J. (2007). “Automatic tuning of PI controllers for an irrigation canal pool.” *Journal of irrigation and drainage engineering*, 133(1), 27–37.
- Ljung, L. and Glad, T. (1994). *Modeling of dynamic systems*. PTR Prentice Hall Englewood Cliffs.
- Matko, D., Geiger, G., and Gregoritz, W. (2000). “Pipeline simulation techniques.” *Mathematics and computers in simulation*, 52(3), 211–230.
- McFarlane, D. and Glover, K. (1992). “A loop-shaping design procedure using H_∞ synthesis.” *IEEE transactions on automatic control*, 37(6), 759–769.
- McFarlane, D. C. and Glover, K. (1990). *Robust controller design using normalized coprime factor plant descriptions*, Vol. 138. Springer.
- Ozdemir, A. A. and Gumussoy, S. (2017). “Transfer function estimation in system identification toolbox via vector fitting.” *IFAC-PapersOnLine*, 50(1), 6232–6237.
- Pham, T. V., Georges, D., and Besançon, G. (2012). “Receding horizon boundary control of nonlinear conservation laws with shock avoidance.” *Automatica*, 48(9), 2244–2251.
- Pintelon, R. and Schoukens, J. (2012). *System identification: a frequency domain approach*. John Wiley & Sons.
- Powell, M. J. (1968). “A fortran subroutine for solving systems of nonlinear algebraic equations.” *Report no.*, Atomic Energy Research Establishment, Harwell, England (United Kingdom).
- Prescott, S. L. and Ulanicki, B. (2008). “Improved control of pressure reducing valves in water distribution networks.” *Journal of hydraulic engineering*, 134(1), 56–65.
- Razvarz, S., Jafari, R., and Gegov, A. (2020). *Flow Modelling and Control in Pipeline Systems: A Formal Systematic Approach*. Springer Nature.
- Razvarz, S., Jafari, R., and Vargas-Jarillo, C. (2019). “Modelling and analysis of flow rate and pressure head in pipelines.” *2019 16th International Conference on Electrical Engineering, Computing Science and Automatic Control (CCE)*, IEEE, 1–6.
- Reddy, H. P., Chaudhry, M. H., and Mohapatra, P. K. (2010). “Modelling of periodic flows in pipelines by transfer function method.” *Journal of Hydraulic Research*, 48(2), 255–259.
- Rugh, W. J. and Shamma, J. S. (2000). “Research on gain scheduling.” *Automatica*, 36(10), 1401–1425.

- Scola, I. R., Besançon, G., and Georges, D. (2018). “Blockage location in pipelines using an implicit nonlinear finite-difference model optimization.” *IFAC-PapersOnLine*, 51(24), 935 – 940.
- Skogestad, S. and Postlethwaite, I. (2007). *Multivariable feedback control: analysis and design*, Vol. 2. Wiley New York.
- Van Pham, T., Georges, D., and Besancon, G. (2014). “Predictive control with guaranteed stability for water hammer equations.” *IEEE transactions on automatic control*, 59(2), 465–470.
- Varga, A. (1991). “Balancing free square-root algorithm for computing singular perturbation approximations.” *Proceedings of the 30th IEEE Conference on Decision and Control*, Brighton, UK, 1062–1065 vol.2 (Dec).
- Weyer, E. (2001). “System identification of an open water channel.” *Control engineering practice*, 9(12), 1289–1299.
- White, F. (2011). *Fluid Mechanics*. McGraw-Hill series in mechanical engineering. McGraw Hill.
- Wylie, E. B. (1965). “Resonance in pressurized piping systems.” *Journal of Basic Engineering*, 87(4), 960–966.
- Zecchin, A. C., Lambert, M. F., Simpson, A. R., and White, L. B. (2010). “Frequency-domain modeling of transients in pipe networks with compound nodes using a laplace-domain admittance matrix.” *Journal of Hydraulic Engineering*, 136(10), 739–755.
- Zecchin, A. C., Simpson, A. R., Lambert, M. F., White, L. B., and Vítkovský, J. P. (2009). “Transient modeling of arbitrary pipe networks by a laplace-domain admittance matrix.” *Journal of Engineering Mechanics*, 135(6), 538–547.